Traction Control for a Rocker-Bogie Robot with Wheel-Ground Contact Angle Estimation

Mongkol Thianwiboon and Viboon Sangveraphunsiri

Robotics and Automation Laboratory, Department of Mechanical Engineering
Faculty of Engineering, Chulalongkorn University,
Phayathai Rd. Prathumwan, Bangkok 10330, Thailand
kieng@eng.chula.ac.th,
viboon.s@eng.chula.ac.th
http://161.200.80.142/mech

Abstract. A method for kinematics modeling of a six-wheel Rocker-Bogie mobile robot is described in detail. The forward kinematics is derived by using wheel Jacobian matrices in conjunction with wheel-ground contact angle estimation. The inverse kinematics is to obtain the wheel velocities and steering angles from the desired forward velocity and turning rate of the robot. Traction Control is also developed to improve traction by comparing information from onboard sensors and wheel velocities to minimize wheel slip. Finally, a simulation of a small robot using rocker-bogie suspension has been performed and simulate in two conditions of surfaces including climbing slope and travel over a ditch.

1 Introduction

In rough terrain, it is critical for mobile robots to maintain maximum traction. Wheel slip could cause the robot to lose control and trapped. Traction control for low-speed mobile robots on flat terrain has been studied by D.B.Reister, M.A.Unseren [2] using pseudo velocity to synchronize the motion of the wheels during rotation about a point. Sreenivasan and Wilcox [3] have considered the effects of terrain on traction control by assume knowledge of terrain geometry, soil characteristics and real-time measurements of wheel-ground contact forces. However, this information is usually unknown or difficult to obtain in practice. Quasi-static force analysis and fuzzy logic algorithm have been proposed for a rocker-bogie robot [4].

Knowledge of terrain geometry is critical to the traction control. A method for estimating wheel-ground contact angles using only simple on-board sensors has been proposed [5]. A model of load-traction factor and slip-based traction model has been developed [6]. The traveling velocity of the robot is estimated by measure the PWM duty ratio driving the wheels. Angular velocities of the wheels are also measured then compare with estimated traveling velocity to estimate the slip and perform traction control loop.

In this research, the method to estimate the wheel-ground contact angle and kinematics modeling of a six-wheel Rocker-Bogie robot are described. A traction control is proposed and integrated with the model then examined by simulation.

A. Bredenfeld et al. (Eds.): RoboCup 2005, LNAI 4020, pp. 682 – 690, 2006.

2 Wheel-Ground Contact Angle Estimation

Consider the left bogie on uneven terrain, the bogie pitch, μ_1, is defined with respect to the horizon. The wheel center velocities v_1 and v_2 parallel to the wheel-ground tangent plane. The distance between the wheel centers is L_B.

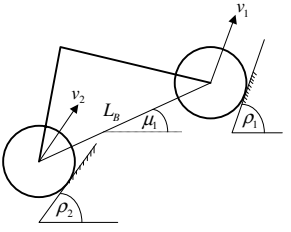

Fig. 1. The left bogie on uneven terrain

The kinematics equations can be written as following

$$v_1 \cos(\rho_1 - \mu_1) = v_2 \cos(\rho_2 - \mu_1) \tag{1}$$

$$v_1 \sin(\rho_1 - \mu_1) - v_2 \sin(\rho_2 - \mu_1) = L_B \dot{\mu}_1 \tag{2}$$

Define $a_1 = L_B \dot{\mu}_1 / v_1$, $b_1 = v_2 / v_1$, $\delta_1 = \rho_1 - \mu_1$ and $\varepsilon_1 = \mu_1 - \rho_2$ then
The contact angles of the wheel 1 and 2 are given by

$$\rho_1 = \mu_1 + \arcsin\left[(a_1^2 - b_1^2)/2a_1\right] \tag{3}$$

$$\rho_2 = \mu_1 + \arcsin\left[(1 + a_1^2 - b_1^2)/2a_1\right] \tag{4}$$

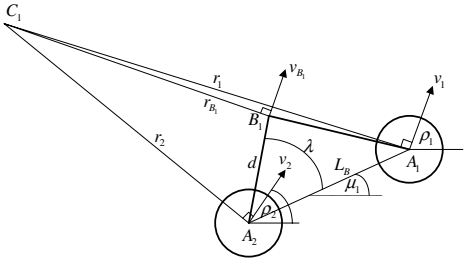

Fig. 2. Instantaneous center of rotation of the left bogie

Velocity of the bogie joint can be written as:

$$v_{B_1} = r_{B_1} \dot{\mu}_1 \tag{5}$$

Consider Left Rocker, the rocker pitch, τ_1, is defined with respect to the horizon direction. The distance between rear wheel center and bogie joint is L_R.

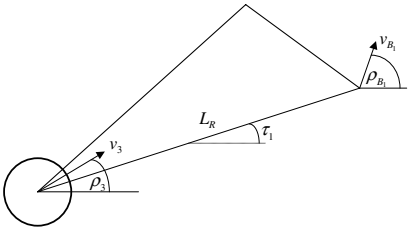

Fig. 3. Left Rocker on uneven terrain

$$\rho_3 = \arccos[(v_{B_1}/v_3)\cos(\rho_{B_1} - \tau_1)] \tag{6}$$

For the right side, the contact angles can be estimated in the same way.

3 Forward Kinematics

We define coordinate frames as in Fig. 4. The subscripts for the coordinate frames are as follows: O: robot frame, D: Differential joint, R_i: Left and Right Rocker ($i = 1,2$), B_i: Left and Right Bogie ($i = 1,2$), S_i: Steering of left front, left back, right front and right back wheels ($i = 1,3,4,6$) and A_i: Axle of all wheels ($i = 1-6$).Other quantities shown are steering angles ψ_i ($i = 1,3,4,6$), rocker angle β, left and right bogie angle γ_1 and γ_2. By using the Denavit-Hartenburg parameters [7], the transformation matrix for coordinate i to j can be written as follows:

$$\mathbf{T}_{j,i} = \begin{bmatrix} C(\eta_j) & -S(\eta_j)C(\alpha_j) & S(\eta_j)S(\alpha_j) & a_jC(\eta_j) \\ S(\eta_j) & C(\eta_j)C(\alpha_j) & -C(\eta_j)S(\alpha_j) & a_jS(\eta_j) \\ 0 & S(\alpha_j) & C(\alpha_j) & d_j \\ 0 & 0 & 0 & 1 \end{bmatrix} \tag{7}$$

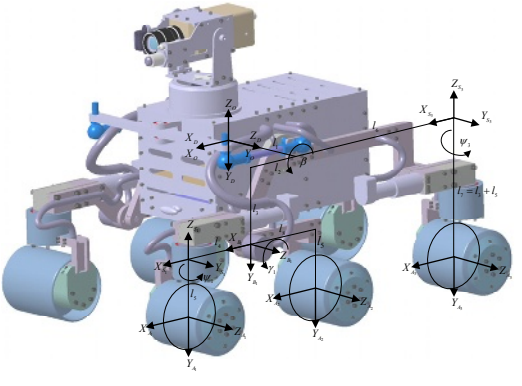

Fig. 4. Robot left coordinate frames

The transformations from the robot reference frame (O) to the wheel axle frames (A_i) are obtained by cascading the individual transformations.

For example, the transformations for wheel 1 are

$$\mathbf{T}_{O,A_1} = \mathbf{T}_{O,D}\mathbf{T}_{D,S_1}\mathbf{T}_{S_1,A_1} \tag{8}$$

To capture the wheel motion, we derive two additional coordinate, contact frame and motion frame. Contact frame is obtained by rotating the wheel axle frame (A_i) about the z-axis followed by a 90 degree rotation about the x-axis. The z-axis of the contact frame (C_i) points away from the contact point as shown in Fig. 5.

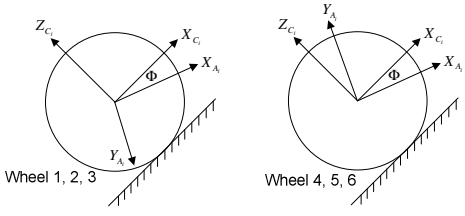

Fig. 5. Contact Coordinate Frame

The transformations for contact frame are derived using Z-X-Y Euler angle

$$\mathbf{T}_{A_i,C_i} = \begin{bmatrix} Cp_iCr_i - Sp_iSq_iSr_i & Cr_iSp_i + Cp_iSq_iSr_i & -Cq_iSr_i & 0 \\ -Cq_iSp_i & Cp_iCq_i & Sq_i & 0 \\ Cr_iSp_iSq_i + Cp_iCr_i & -Cp_iCr_iSq_i + Sp_iSr_i & Cq_iCr_i & 0 \\ 0 & 0 & 0 & 1 \end{bmatrix} \tag{9}$$

The wheel motion frame is obtained by translating along the negative z-axis by wheel radius (R_w) and translating along the x-axis for wheel roll ($R_w\theta_i$).

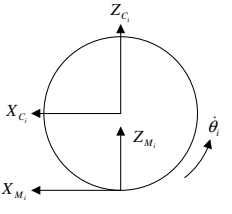

Fig. 6. Wheel Motion Frame

The transformation matrices for the front left wheel can be written as (10) and the transformation for other wheels can be written in the same way.

$$\mathbf{T}_{O,M_1} = \mathbf{T}_{O,D}\mathbf{T}_{D,B_1}\mathbf{T}_{B_1,S_1}\mathbf{T}_{S_1,A_1}\mathbf{T}_{A_1,C_1}\mathbf{T}_{C_1,M_1} \tag{10}$$

To obtain the Jacobian matrices, the robot motion is express in the wheel motion frame, by applying the instantaneous transformation $\dot{\mathbf{T}}_{\hat{O},O} = \mathbf{T}_{\hat{O},\hat{M}_i}\dot{\mathbf{T}}_{M_i,O}$

$$\dot{\mathbf{T}}_{\hat{O},O} = \begin{bmatrix} 0 & -\dot{\phi} & \dot{p} & \dot{x} \\ \dot{\phi} & 0 & -\dot{r} & \dot{y} \\ -\dot{p} & \dot{r} & 0 & \dot{z} \\ 0 & 0 & 0 & 1 \end{bmatrix} \tag{11}$$

where ϕ, p, r = yaw, pitch, row angle of the robot respectively.

Once the instantaneous transformations are obtained, we can extract a set of equations relating the robot's motion in vector form $[\dot{x} \quad \dot{y} \quad \dot{z} \quad \dot{\phi} \quad \dot{p} \quad \dot{r}]^T$ to the joint angular rates. The results of the left and right front wheel are found to be

$$\begin{bmatrix} \dot{x} \\ \dot{y} \\ \dot{z} \\ \dot{\phi} \\ \dot{p} \\ \dot{r} \end{bmatrix} = \begin{bmatrix} A_i & 0 & B_i & C_i \\ D_i & 0 & E_i & F_i \\ G_i & 0 & H_i & I_i \\ 0 & 0 & 0 & J_i \\ 0 & -1 & -1 & 0 \\ 0 & 0 & 0 & K_i \end{bmatrix} \begin{bmatrix} \dot{\theta}_i \\ \dot{\beta} \\ \dot{\gamma}_i \\ \dot{\psi}_i \end{bmatrix} \qquad i = 1,4 \tag{12}$$

The results of wheel 2 and 5 (the left and right middle wheel) are found to be

$$\begin{bmatrix} \dot{x} \\ \dot{y} \\ \dot{z} \\ \dot{\phi} \\ \dot{p} \\ \dot{r} \end{bmatrix} = \begin{bmatrix} A_i & 0 & B_i \\ C_i & 0 & 0 \\ D_i & 0 & E_i \\ 0 & 0 & 0 \\ 0 & -1 & -1 \\ 0 & 0 & 0 \end{bmatrix} \begin{bmatrix} \dot{\theta}_i \\ \dot{\beta} \\ \dot{\gamma}_i \end{bmatrix} \qquad i = 2,5 \tag{13}$$

The results of wheel 3 and 6 (the left and right back wheel) are found to be

$$\begin{bmatrix} \dot{x} \\ \dot{y} \\ \dot{z} \\ \dot{\phi} \\ \dot{p} \\ \dot{r} \end{bmatrix} = \begin{bmatrix} A_i & 0 & B_i \\ C_i & 0 & D_i \\ E_i & 0 & F_i \\ 0 & 0 & G_i \\ 0 & -1 & 0 \\ 0 & 0 & H_i \end{bmatrix} \begin{bmatrix} \dot{\theta}_i \\ \dot{\beta} \\ \dot{\psi}_i \end{bmatrix} \qquad i = 3,6 \tag{14}$$

The parameters A_i to K_i in the matrices above can be easily derived in terms of wheel-ground contact angle $(\rho_1,..,\rho_6)$ and joint angle $(\beta, \gamma, \text{and } \psi)$.

4 Wheel Rolling Velocities

Consider forward kinematics of the front wheel (12), define $\dot{x}_d$ as the desired forward velocity and $\dot{\phi}_d$ as desired heading angular rate. The 1st and 4th equation give

$$\begin{aligned} \dot{x}_d &= A_i\dot{\theta}_i + B_i\dot{\gamma}_i + C_i\dot{\psi}_i \\ \dot{\phi}_d &= J_i\dot{\psi}_i \end{aligned} \qquad i = 1,3 \tag{15}$$

The rolling velocities of the front wheels can be written as

$$\dot{\theta}_i = (\dot{x}_d - B_i\dot{\gamma}_i - \frac{C_i}{J_i}\dot{\phi}_d)/A_i \qquad i = 1,3 \tag{16}$$

Similarly, the rolling velocities of the middle and rear wheels can be written as

$$\dot{\theta}_i = (\dot{x}_d - B_i\dot{\gamma}_i)/A_i \qquad i = 2,5 \tag{17}$$

$$\dot{\theta}_i = (\dot{x}_d - \frac{B_i}{G_i}\dot{\phi}_d)/A_i \qquad i = 3,6\,. \tag{18}$$

5 Slip Ratio

In section 3 and 4, we assume that there is no side slip and rolling slip between wheel and ground. Then slip must be minimizing to guarantee accuracy of the kinematics model. The slip ratio S, of each wheel is defined as follows:

$$S = \begin{cases} (r\dot{\theta}_w - v_w)/r\dot{\theta}_w & (r\dot{\theta}_w > v_w : accelerating) \\ (r\dot{\theta}_w - v_w)/v_w & (r\dot{\theta}_w < v_w : decelerating) \end{cases} \tag{19}$$

where r = radius of the wheel
θ_w = rotating angle of the wheel
$r\dot{\theta}_w$ = wheel circumference velocity
v_w = traveling velocity of the wheel

S is positive when the robot is accelerating and negative when decelerating. The robot can travel stably when the slip ratio is around 0 and will be stuck when the ratio is around 1. By measuring of the wheel angles with information from the accelerometer, we can minimize slip so the traction of the robot is improved.

In the traction control loop, a desired slip ratio S_d is given as an input command. The feedback value $\hat{S}$ is computed from a slip estimator. To complete the estimation of the slip, we need the rolling velocity and the traveling velocity of the wheels, ω and v_w. Rolling velocity of the wheels is easily obtained from encoders which installed in all wheels. Traveling velocity of the wheel can be computed from robot velocity by using data from onboard accelerometer.

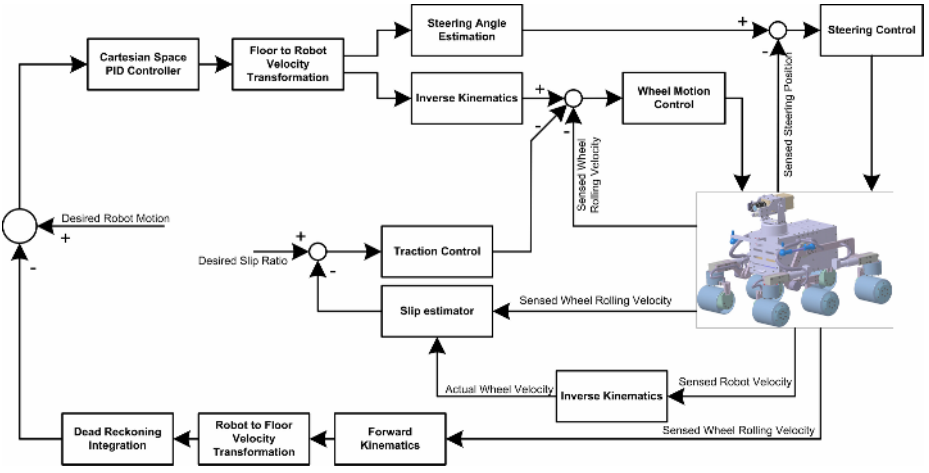

Fig. 7. Robot Control Schematic

6 Experiment

The system was verified in Visual Nastran 4D. In Fig. 8, the robot climbs up a 30-degree slope, with coefficient of friction 0.5. Without control, the robot move at 55 mm/s, then the front wheels touched the slope at $t = 0.5$ sec. and begin to climb up. Robot velocity reduced to 25 mm/s. But the robot continues to climb until the middle wheels touch the slope at $t = 9$ sec. The velocity reduced to nearly zero. With control, the sequence was almost the same until $t = 0.5$ sec. Then the velocity reduced to 35 mm/s when the front wheels touched the slope. The middle wheels touched the slope at $t = 6$ sec. and velocity reduced to 28 mm/s. Both back wheels begin to climb up the slope at $t = 15$ sec. with velocity approximately 20mm/s.

In Fig. 9, the robot traversed over a 32mm depth and 73mm width ditch with coefficient of friction about 0.5. The robot move at 55 mm/s, then the front wheels went down the ditch at $t = 0.5$ sec. and begin to climb up when front wheels touch the

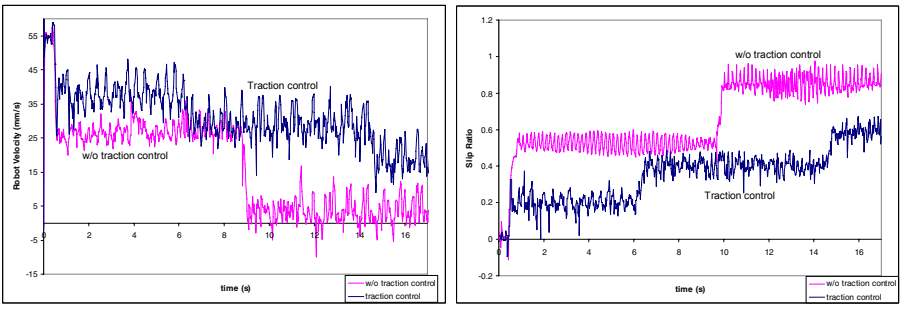

Fig. 8. Velocity and Slip ratio when climbed up 30 degrees slope

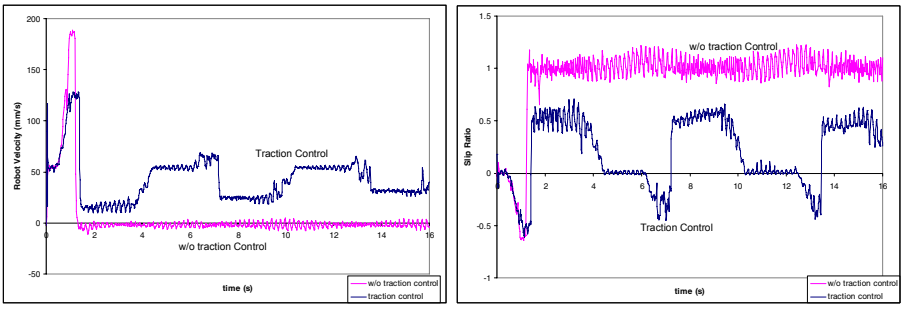

Fig. 9. Velocity and Slip ratio when traversed over a ditch

up-edge of the ditch. But the wheels slipped with the ground and failed to climb up. Then the slip ratio went up to 1 ($S = 1$), the robot has stuck at $t = 1.5$ sec.

With traction control, after the front wheels went down the ditch, the slip ratio was increased. Then the controller tried to decelerate to decrease the slip ratio. When the slip ratio was around 0.5, the robot continued to climb up. Until $t = 4.5$ sec., both of the front wheels went up the ditch completely and the robot velocity increased to the 55 mm/s as commanded. At $t = 6$ sec., the middle wheels went down the ditch. The robot velocity also increased temporary and back to 55 mm/s again when the middle wheels went up completely. The last two wheels went down the ditch at $t = 13$ sec. and the sequence was repeated in the same way as front and middle wheels.

8 Conclusion

In this research, the wheel-ground contact angle estimation has been presented and integrated into a kinematics modeling. Unlike the available methods that applicable to the robots operating on flat and smooth terrain, the proposed method uses the Denavit-Hartenburg notation like a serial link robot, due to the rocker-bogie suspension characteristics. A traction control is proposed based on the slip ratio. The slip ratio is estimated from wheel rolling velocities and the robot velocity. The traction control strategy is to minimize this slip ratio. So the robot can traverse over obstacle without being stuck. The traction control is verified in the simulation with two conditions. Climbing up the slope and moving over a ditch with coefficient of friction 0.5. The robot velocity and slip ratio are compared between using traction control and without using traction control system.

References

1. JPL Mars Pathfinder. February 2003. Available from: http://mars.jpl.nasa.gov/MPF
2. D.B.Reister, M.A.Unseren: Position and Constraint force Control of a Vehicle with Two or More Steerable Drive Wheels, IEEE Transaction on Robotics and Automation, page 723-731, Volume 9 (1993)

3. S.Sreenivasan, B.Wilcox: Stability and Traction control of an Actively Actuated Micro-Rover, Journal of Robotic Systems (1994)
4. H.Hacot: Analysis and Traction Control of a Rocker-Bogie Planetary Rover, M.S. Thesis, Massachusetts Institute of Technology, Cambridge, MA (1998)
5. K.Iagnemma, S.Dubowsky: Mobile Robot Rough-Terrain Control (RTC) for Planetary Exploration, Proceedings of the 26th ASME Biennial Mechanisms and Robotics Conference, Baltimore, Maryland (2000)
6. K.Yoshida, H.Hamano: Motion Dynamics of a Rover with Slip-Based Traction Model, Proceeding of 2002 IEEE International Conference on Robotics and Automation (2002)
7. John J. Craig: Introduction to Robotics Mechanics and Control, Second Edition, Addison-Wesley Publishing Company (1989)
8. M.Thianwiboon, V.Sangveraphunsiri, R.Chancharoen: Rocker-Bogie Suspension Performance, Proceeding of the 11th International Pacific Conference on Automotive Engineering (2001)